

## Biomechanics and Traditional Use of *Raphia matombe* Rachis in Northern Angola

Thea Lautenschläger,<sup>a,\*</sup> Andreas Kempe,<sup>a,b</sup> Katharina Bunk,<sup>c</sup> Monizi Mawunu,<sup>d</sup> and Christoph Neinhuis<sup>a</sup>

The huge rachis of *Raphia matombe* is intensely used by local people in Northern Angola for the construction of stools, chairs, shelves, beds, or baskets. This is not only because it is a charming, fast-growing, renewable, and locally abundant material with a high aesthetic value but also due to its extremely light weight structure. Nevertheless, up to now the anatomical and mechanical features of rachises have hardly been studied, although monocotyledonous stem tissues have been the subject of numerous papers. This study presents an analysis of the rachis of *Raphia matombe* and its material gradients over its whole length and cross-sectional area. The modulus of elasticity increased from the inner towards the outer layers, whereas no clear axial gradient from the base to the apex was found. However, the specific modulus of elasticity increased from the base to the apex in relation to the density, reaching maximum values of 19.0 MPa/kgm<sup>-3</sup>. Still, the high anatomical and mechanical heterogeneity of the rachis impede quick and easy processing.

*Keywords:* Biomechanics; Composite material; Density; Specific modulus of elasticity; Angola

*Contact information:* a: Department of Biology, Institute of Botany, Faculty of Science, Technische Universität Dresden, 01062 Dresden, Germany; b: Institute of Lightweight Engineering and Polymer Technology, Faculty of Mechanical Science and Engineering, Technische Universität Dresden, 01307 Dresden, Germany; c: Plant Biomechanics Group & Botanic Garden, University of Freiburg, 79104 Freiburg/Breisgau, Germany; d: Department of Agronomy, Kimpa Vita University, Uíge, Angola; \* Corresponding author: thea.lautenschlaeger@tu-dresden.de

### INTRODUCTION

Palms, which belong to the Monocotyledons, do not produce real wood. Nevertheless, they can withstand high static and dynamic loads (e.g., during hurricanes), up to a certain point. Their primary fiber bundles, which are embedded in the parenchymatous ground tissue and form a natural composite, are responsible for this high load-bearing capacity. The texture and toughness of this composite largely depend upon the distribution of vascular bundles and the amount of sclerenchyma present (Parthasarathy and Klotz 1976). While peripheral crowded bundles provide most of the mechanical strength of the stem due to their large fiber caps, the lacunose center of the stems consists of widely separated bundles embedded in spongy, nonlignified ground tissue (Tomlinson 2006). According to Rich (1987a,b), the palm stem density, modulus of elasticity, and modulus of rupture are the highest in the periphery and base due to sclerification of the fiber bundles. Furthermore, a gradual decrease in stiffness could be observed across the fiber cap towards the surrounding parenchymatous tissue (Rüggeberg *et al.* 2008). However, the anatomical features were found not only for stems, but also for palm petioles (Parthasarathy and Klotz 1976). In contrast to the petioles of simple and palmate leaves, the petiole of pinnate leaves function in an analogous manner to the branches supporting

separate leaves, so that their flexural stiffness increases towards the base (Niklas 1971).



**Fig. 1.** (a) *Raphia matombe* in its natural swampy habitat in northern Angola. The palm forms only short stems; (b) the leaves rank as the longest in plant kingdom and are pinnately compound (c)

Leaves of the genus *Raphia* are pinnately compound and are the longest in the plant kingdom, with a length of up to 10 m. In northern Angola's Uíge Province, *Raphia matombe* De Wild. (Figs. 1a, 1b, and 1c) is extensively used for the extraction of palm wine 'matombe' (Monizi *et al.* 2018a), or for breeding of the edible larvae of *Rhynchophorus phoenicis*, which feed on damaged rachises (Lautenschläger *et al.* 2017). In addition, the leaf rachis, leaflets, and the fibers of the leaf-base are used in different ways, for example, for furniture and construction material (Figs. 2a, 2b, and 2c) (Lautenschläger *et al.* 2018, Monizi *et al.* 2018b). Palm "wood" generally is not used because it is neither homogenous nor does it provide adequate mechanical properties. The current study focused on the structural properties of the rachis, as this material is extremely light and very stable, which allows its intensive usage by local people for traditional furniture. In the local Bakongo language Kikongo, the palm is called 'matombe' while the vernacular Portuguese name for the palm is 'bordão'. The plants grow in swampy areas and wetlands along rivers and creeks, which are frequently found in the mosaic-like structure of the Zambesi-Guinense forest and savannah formations. Leaves arise close to the ground from the base of a comparatively short stem. According to the local people, the palms are abundant and therefore provide an always available and cheap material, which is easy to harvest. However, detailed studies on the number of leaves produced per year are still lacking. The leaves are cut and dried for use as construction material. Depending on the mechanical stress the respective furniture is exposed to, local producers use a machete to cut the unequal cross-sections of the rachis into the desired form. For small stools used in the street markets, the outer part of rachis is cut away to form a rectangular shape which can be processed more easily. In the case of large bed frames, the strong outer part remains.



**Fig. 2.** Furniture such as tables (a) or stools (b) made of *Raphia matombe* rachis. Nails as connecting element are manufactured from the outer part of the rachis (c)

The mechanical properties of plant material depend on physical, chemical, and morphological characteristics such as density, chemical composition, or tissue distribution. Therefore, morphological, biomechanical, and chemical analyses of the relevant tissues were carried out at different positions along the rachis of *Raphia matombe* as well as across the cross-section to address the following questions:

- Does the *Raphia* rachis show similar anatomical and mechanical properties as palm stems?
- Is the rachis an appropriate material for general construction components?
- Is the material a potential hardwood substitute?

## PROPERTIES ASSESSMENT

### Material Collection

Plant material was collected in Angola's Northern Uíge Province, where *Raphia matombe* is abundant and widely used. The two leaves investigated here were freshly cut 1 m above the ground and had a length of about 8 m. In order to transport the material to Germany, these two complete leaves were cut into five segments each with a length of approx. 1.4 m. All leaflets were removed.

## Methods

### *Morphological and anatomical analysis*

Different methods were used to describe the morphology as well as the anatomy of the *Raphia matombe* rachis. To reconstruct changes in the geometry of the cross-section along the leaf, one 1-cm-thick slice of each segment was cut off at the beginning and at the tip of the leaf. The surfaces of all slices were smoothed manually with sand paper and scanned with a scanner camera (Pentacon Scan 6000S, LaserSoft Imaging AG, Kiel, Germany) to document the different shapes as well as the distribution of the vascular bundles. To quantify the number of vascular bundles over the cross-section as well as along the whole rachis, these slices were classified into three zones: outside, inside, and transition zones (Fig. 4a). The transition zone showed the shift to the inside zone, which is characterized by large bundles with thin cell walls. The bundles were counted and extrapolated to an area of 1 cm<sup>2</sup> to compare the data. The area of the cross-sections was determined *via* GIMP by counting pixels with the counting function (after posterization to two tones and using images with a resolution of 700 dpi).

For further details, pictures were taken at larger magnifications with a reflected light microscope (Olympus SZX16, Jena, Germany). For microscopic analysis, parts of the rachis were cut into small pieces and incubated in hot water for approximately half an hour in order to obtain thin sections using razor blades. The samples were analyzed without staining using a light microscope (Carl Zeiss Axioskop 2, Jena, Germany). The thickness of ten sclerenchyma layers surrounding the vascular bundles was measured with a measuring eyepiece in the ocular, to compare the differences in the outer, inner, and transitions zone.

To complete the microscopic analysis of the rachis, the samples were investigated with a scanning electron microscope (Carl Zeiss Supra40VP, Jena, Germany). These pictures can give an insight into the cross-sectional area as well as into the longitudinal organization.

### *Chemical composition*

For a comparison of the chemical composition along the leaf rachis, samples from segment 1 and segment 4 were broken into small pieces with a hammer and milled to a fine powder. The dry weight of the powder was determined automatically in a moisture indicator (KERN MLS 50-3HA 160N, KERN & SOHN, Balingen-Frommern Germany), by filling approximately 0.5 g into the device. The powder was then automatically heated and weighed.

The cellulose contents were investigated as described by Kuerschner and Hoffer (1931), the lignin contents according to Theander and Westerlund (1986). Toluene-ethanol extraction was used to analyze residual extracts content within the rachis. The chemical analyses took place at the Institute of Wood and Plant Chemistry of the Technische Universität Dresden in Germany.

The moisture content of samples was determined according to DIN EN 13183. Therefore, 10 cm long specimens of the whole rachis from the basal segment 0, from the middle segment 3 and from the apical segment 5 were weighed fresh, after drying for two months at room temperature and a humidity of 40% (KERN EMB 100-3, KERN & SOHN, Balingen-Frommern Germany), and after kiln drying (Binder ED 240, Tuttlingen, Germany). The moisture content is given for the fresh samples and the samples used in the mechanical test set up. It is calculated by dividing the mass of the lost water by the mass of the dried sample multiplied by 100%.

### *Mechanical analysis*

First, the flexural rigidities of entire rachis segments in their fresh state were determined by a three-point bending test within the elastic range. Therefore, within 2 h of harvesting, the segments were placed between two vertical supports and then loaded by hanging materials of varying weight from the middle of the rachis. Dial extensometers, one of which was in the middle and one at every support, measured the deflection of the rachis in the middle, and recognized deflections at the supports. These were remeasured in a dry state in Dresden.

Back in Germany, all segments were cut into specimens, which were subjected to bending, compression, and tension tests using a Zwickiline Z2.5 (Zwick GmbH, Ulm, Germany). Tests were performed in accordance with DIN EN ISO 527 (2012) and ISO 13061 (2014) but with modified dimensions of specimens due to the rachis size. The testing machine was equipped with a 50 N load cell for tension tests of extracted vascular bundles and a 1 kN load cell for bending and compression tests of specimens. The testing speed for the bending, compression, and tension tests was set to 2 mm/min. The dimensions of the samples were measured using a caliper (TopCraft). All tests were conducted at constant room temperature (22 °C). The moduli of elasticity were calculated from the slope of the initial linear part of the stress-strain curve. In addition, the ultimate tensile strength and breaking strain of the vascular bundles were determined in tension tests.

Due to its highly anisotropic character, which is further explained in the morphological part of the results, three different layers of the cross-section were defined: the outer layer, which was approximately 1 mm in thickness, the transition layer with a similar thickness, and the inner layer, which made up the main part of the cross-section (Fig. 4a). Thin specimens were prepared from these three layers using a fine saw to conduct three-point bending tests. To determine a gradient in the material parameters over the cross-section and along the rachis, between 34 and 50 specimens were cut at each of the four segments from the leaf base towards the apex, except at the apical segment, as the outside and transition layers were too thin to yield suitable specimens. The specimens were cut to dimensions of 1 mm x 13 mm x 120 mm. Each specimen was measured individually before testing, and due to preparation process, the true width and height were  $13.3 \pm 1.8$  mm and  $1.13 \pm 0.15$  mm, respectively. The test direction was perpendicular to the flat side.

For the compression tests, cubes with dimensions of 5 mm x 5 mm x 5 mm were cut from all five segments of the rachis. The authors aimed to prepare 30 cubes at each position, but only a smaller sample number could be prepared from the apical segment. The desired dimensions of the samples could not always be met accurately, due to irregularities in the plant material and shape. Therefore, each specimen was measured individually before testing, and an accuracy of  $5.02 \pm 0.39$  mm was achieved. Compression tests were performed in axial direction. Due to the preparation of the specimens, only an outer zone comprised of the previously defined outside and transition layers could be tested in comparison to the inside tissue.

To identify the influence of the vascular fiber bundles to the strengthening of the tissue, the bundles were separated from the surrounding parenchymatous tissue. For this, the middle part of the leaf (Segment 3) was cut lengthwise using a fine saw and then six bundles were extricated manually, resulting in a total of 30 samples with an average diameter of  $1.32 \pm 0.28$  mm. The remaining parenchymatous cells around the exposed bundles were removed with sandpaper.

### Density

The samples, which were later used for mechanical tests, were previously used to determine the density gradient. Therefore, 20, 30, and 45 specimens from outside, transition, and inside layers prepared for bending tests were used, plus 93 specimens from inside, which were prepared for compression tests. Because the samples originated from five different positions along the leaf, a potential density gradient along the leaf was additionally investigated. The height, width, and depth of each piece was measured with a caliper from 'Topcraft' to calculate the volume. These measurements were conducted at three positions of the specimen and averaged, to exclude errors arising from small irregularities of the shape. Afterwards, all samples were weighed with a special accuracy-weighing machine (Ohaus Adventurer).

For the comparison of fresh and dry material, the densities of 24 freshly cut samples of one rachis were determined in the same manner as above during the field trip to Uíge/Angola. All pieces were transported to Dresden and stored at room temperature for one month. Afterwards, all samples were measured and weighed again. Additional determination of the dimensions was necessary, because the material shrank during drying. With this data, the fresh and dry density of the samples was calculated and compared.

## RESULTS AND DISCUSSION

### Morphological and Anatomical Analysis

The picture series of the rachis pieces along Leaf 1 (Positions 1-5 plus 1 piece at the tip) shows the change in the cross-sectional geometry (Fig. 3). All pictures represent the real size relations and are presented with the adaxial side upwards to reflect the rachis in its natural habitus. At the leaf base, the rachis was even more U-shaped than in the first cross-sectional picture of the scan series. At approximately two meters above the cut of the first rachis segment, the shape of the cross-section changed slightly from a U-shape to an oval. Beginning with the part bearing leaflets, the adaxial side changed from concave into a convex triangular shape, while the abaxial side remained round. In addition to the change in geometry, the rachis tapered down towards its apex. The basal segment had a maximum width and height of about 70 mm at the cut towards the ground, whereas the last segment had a maximum width of only 15 mm at the cut.

In addition to the change of the rachis geometry along the leaf, the shape, distribution, and size of vascular bundles changed along the cross-section of the *Raphia* rachis (Fig. 4a). The cross-section of the rachis showed the typical vascular bundle distribution of monocotyledonous stems, specifically of Arecaceae as they are incapable of secondary growth. The number of vascular bundles was low at the center and at the base and increased considerably towards the periphery and the apex (Fig. 3 and Fig. 4).

Additionally, the shapes and dimensions of the vascular bundles changed with their position in the cross-section. In the inner region, they were round, except for a small tip at the position of the metaxylem. The vascular bundles that were closer to the periphery elongated to become oval. The outermost vascular bundles almost looked like wedges of different sizes and were arranged alternately to perfectly fill all interspaces, leaving almost no parenchyma tissue in between. Furthermore, the vascular bundles also decreased in size towards the outer layer (Fig. 4a).

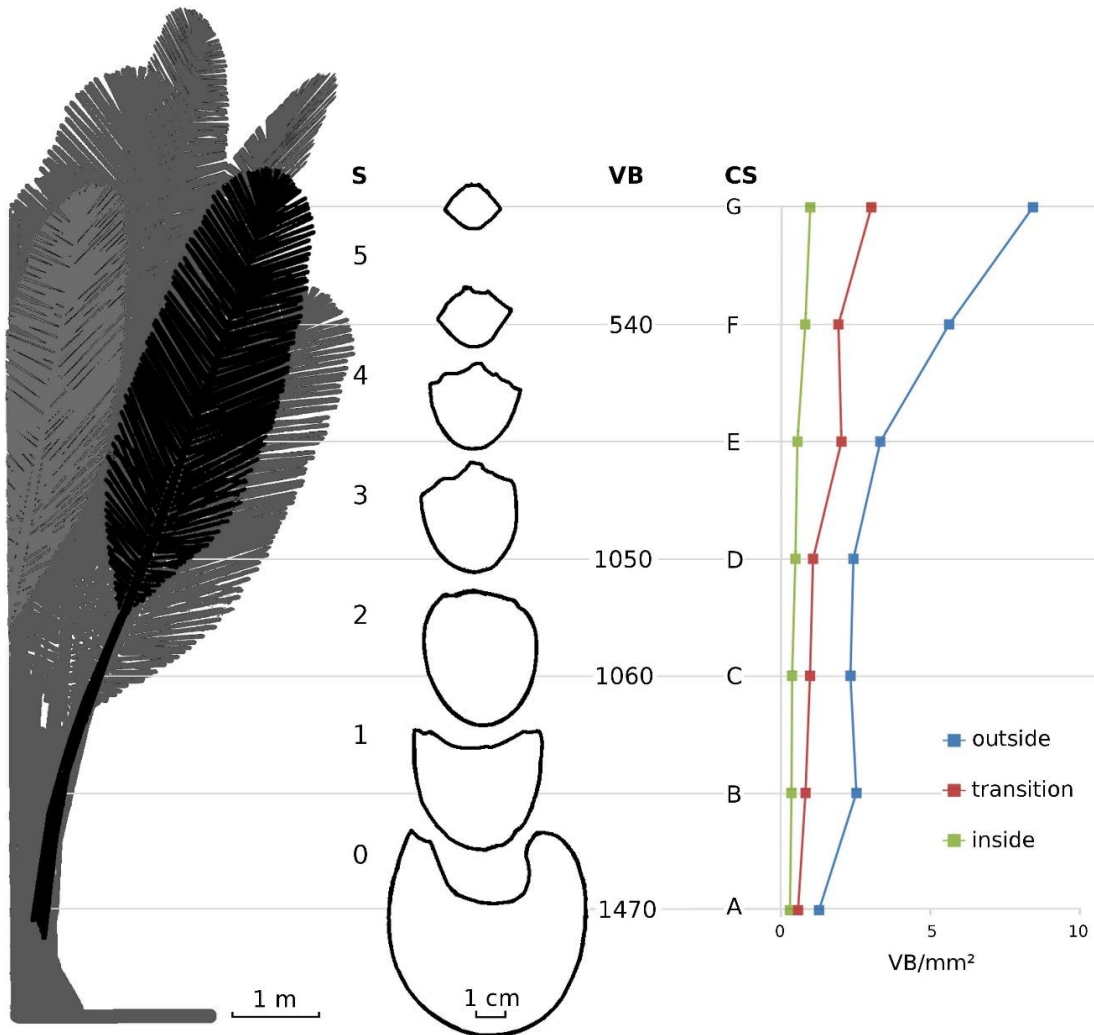


**Fig. 3.** Definition of segments and cross sections along the leaf rachis, their total number of vascular bundles and the gradient of vascular bundles in the different layers, converted to mm<sup>2</sup>. CS = cross-section (A-G), S = segment number, VB = total number of vascular bundles across the whole cross-section

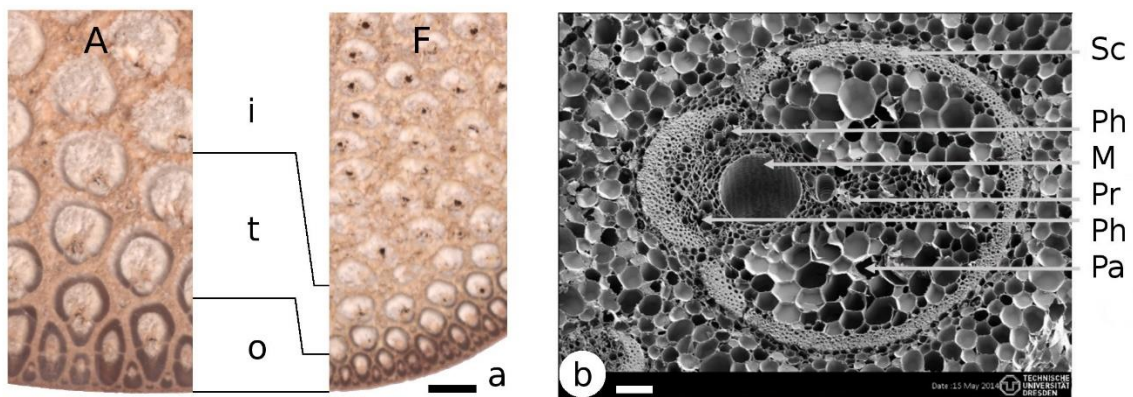


**Fig. 4.** (a) Part of the cross-section (A and F) of the rachis with clearly visible fiber bundles. Definition of three different layers over the cross-section: outside (o), transition (t), and inside layer (i); scale bar 500 µm. (b) SEM image of vascular bundle of the inner part of the cross section; M = metaxylem, Pa = parenchyma, Ph = phloem, Pr = protoxylem, Sc = sclerenchyma; scale bar 100 µm

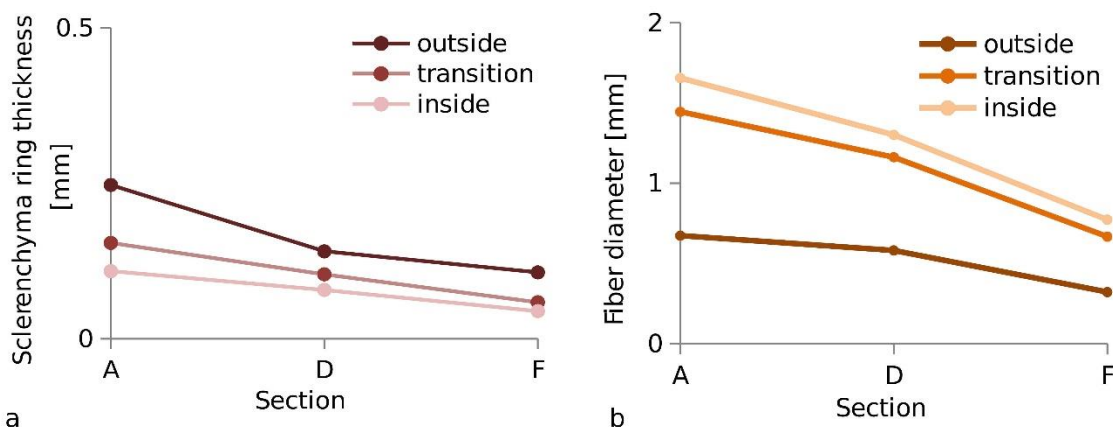


**Fig. 5.** (a) Diameter of vascular bundles and (b) thickness of the sclerenchymatous ring with respect to location within cross-section and along the rachis based on three sections A, D, and F

The thickness of the sclerenchyma layer, embracing the vascular bundles, increased constantly from the inside towards the outside region of the rachis (Fig. 4a and 5). While the thickness in the inner region was between  $109 \pm 25 \mu\text{m}$  at section A and  $45 \pm 7 \mu\text{m}$  at section F, it increased to  $247 \pm 105 \mu\text{m}$  in the outside layer at section A and  $107 \pm 46 \mu\text{m}$  at section F (10 measurements per category). In addition, the diameter of the fiber bundles changed along the rachis and within the section (Fig. 4). The bundles were thickest in the inner region at the base ( $1.66 \pm 0.08 \text{ mm}$ ) and decreased towards the outside at the apex ( $0.32 \pm 0.13 \text{ mm}$ ). Only the peripheral widths of outside bundles were used in the comparison.

In Figure 4 B, the SEM-image of a cross-sectional cut through the vascular bundle of the inner part of the *Raphia* rachis shows the big vessel of the metaxylem and the conspicuous ring-shaped sclerenchyma. The area of the protoxylem can be recognized near the big metaxylem vessel. All conducting elements were embedded in a huge amount of parenchymatous tissue. The sclerenchymatous ring surrounded nearly all the conducting tissue and had only two very thin gaps. Sclerenchymatous caps are well known to protect vessels in monocots from stronger stresses and deformations. In contrast to the observations in *Washingtonia robusta*, with both the cell wall area fraction and cell wall thickness decreasing from its center to the periphery of the fiber cap (Rüggeberg *et al.* 2008), here, an increase of the latter from the inner to the outer part of the fiber ring was observed.

### Chemical Composition

The average chemical composition (lignin, cellulose, hemicellulose, extractives) of the rachis at the base (cross-section B) and near the apex (cross-section E) was the same. Lignin, cellulose, and hemicellulose had proportions of  $21.1 \pm 0.0\%$ ,  $39.2 \pm 0.2\%$ , and  $33.5 \pm 0.2\%$ . The extractives had a proportion of  $6.5 \pm 1.8\%$ .

The moisture content of the fresh samples was higher in the basal segment 0 ( $256 \pm 16\%$ ) than in segment 3 ( $158 \pm 5\%$ ), or above all in the apical segment 5 ( $126 \pm 0.2\%$ ). The air-dried specimens of all the tested segments exhibited a moisture content of  $8 \pm 1\%$  in average. The decrease from base to apex could be explained by the fact that the proportion of the parenchymatous tissue is higher at the base and therefore during the drying process is losing more water than the apical part of the rachis. The correlation

between moisture content and the amount of parenchymatous tissue can also be observed in other monocotyledons. Thus, the moisture content of *e.g.* coconut palm stem increases with stem height (Killmann 1983) because here the apical part contains more parenchyma than the dense stem base.

## Density

By classifying samples in reference to their location within the cross-section, the density of the three different groups differed considerably (Table 1). The samples taken from the outside layer exhibited an average dry density of  $607 \pm 138 \text{ kgm}^{-3}$ ; those from the transition zone had an average dry density of  $369 \pm 76 \text{ kgm}^{-3}$ , which represented 60% of the density in the outer layer. In the central region, the value again decreased to  $194 \pm 52 \text{ kgm}^{-3}$ , representing only 32% of the density of the outside layer. The values showed a gradual decrease in density from the outside towards the inside layer at each position (Fig. 6a). For the samples taken from the outside layer, the density along the leaf was not significantly different (Tukey–Kramer test,  $P > 0.05$ ), whereas the values of the transition and inside layer showed a significant increase of 46% and 59% between segments 1 and 5. These data differ from those of other studies on palm wood density distributions (Rich 1986).

Density depended also on maturity. Without considering gradients along the rachis, the fresh and dried segments showed densities of only  $294 \pm 75 \text{ kgm}^{-3}$  and  $202 \pm 56 \text{ kgm}^{-3}$  respectively, representing a water content of 31%. The density of younger tissue was lower than in older ones, substantiating earlier results from studies of these stems (Rich 1987).

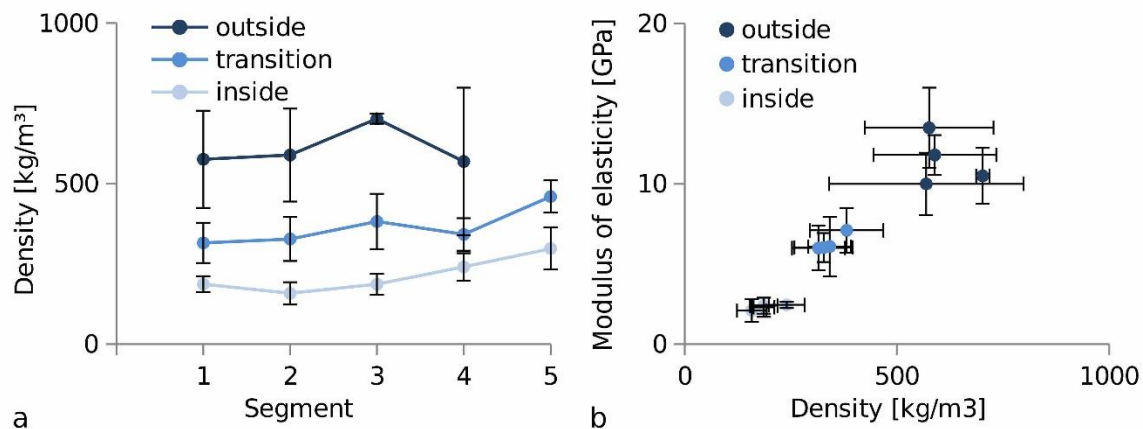


**Fig. 6.** (a) Dry density in the outside, transition, and inside layer at four positions along the entire *Raphia* rachis and across its cross-section; (b) Correlation of modulus of elasticity from bending tests and dry density along the rachis

## Mechanical Analysis

Different test sets were conducted to classify the materials' properties according to their gradient of modulus of elasticity along and across the rachis.

### Three-point bending tests of entire rachis segments

The three-point bending test of segments of the entire rachis showed an increasing structural modulus of elasticity from the base to the apex (Fig. 7a). The structural modulus of elasticity was the lowest in the 1<sup>st</sup> segment of the fresh leaves with 2.9 GPa and 3.8 GPa and increased almost linearly up to 5.6 GPa in the 4<sup>th</sup> segment. Furthermore, the structural

moduli of elasticity increased for all pieces after drying by 43% on average, up to 5.3 GPa for segment 1 and up to 7.8 GPa for segment 4.

The structural modulus of elasticity is a value that only gives an orientation in comparison to wood, a much more homogeneous material than the palm rachis, assuming a full cross-section and neglecting the material gradient inside. The increase of the structural modulus of elasticity can easily be explained by the proportion of the stiff outside layer to the entire cross-section. Smaller cross-sections lead to a higher proportion of the outside layer, with its higher Young's modulus, than the inside layer. Thus, the structural modulus of elasticity increased as shown in correlation to the cross-sectional dimensions. However, the dimensions in cross-section at the base led to a great second moment of inertia, resulting in sufficient flexural rigidity.

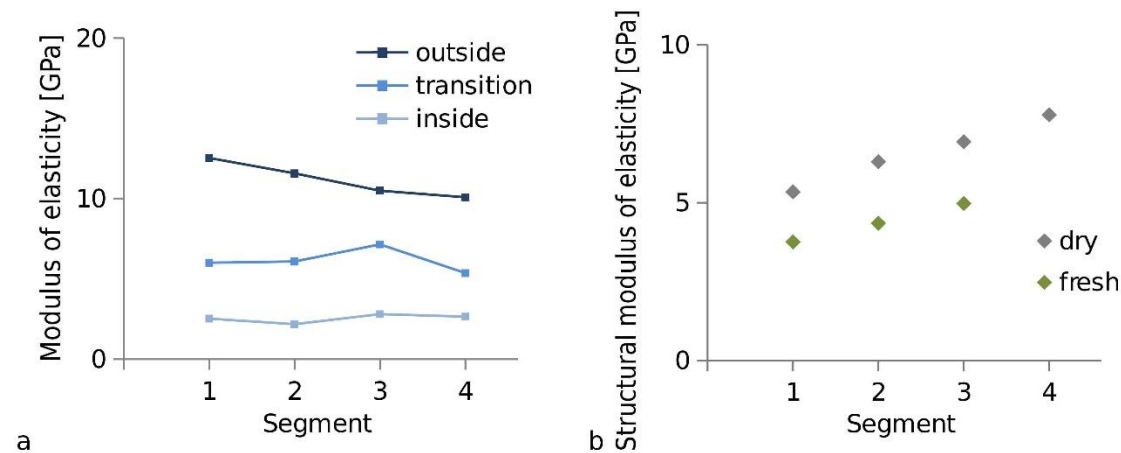


**Fig. 7.** (a) Modulus of elasticity of bending specimens according to the position across the cross-section and along the rachis; (b) Structural modulus of elasticity of entire segments along the rachis, comparing fresh and dry samples

### Three-point bending tests of rachis specimens

In addition to the difference of the modulus of elasticity under fresh and dry conditions, three-point bending tests to identify a potential gradient along the leaf and over the cross-section were conducted under dry conditions, as summarized in Fig. 7b. At all positions, the modulus of elasticity decreased gradually from the outside layer (11.7 GPa in average) towards the transition (6.3 GPa in average) and the inside layer (2.5 GPa in average). At cross-section F (apex), the rachis already had a diameter that was too small to differentiate between samples from the outside, transition, and inside layer.

No gradient in modulus of elasticity along the rachis was measured in the samples from the transition and inside layer, in contrast to the outside layer, in which the modulus decreased slightly but not significantly (Tukey–Kramer test,  $P > 0.05$ ). However, this decrease can also be explained by the discrepancy between the thickness of specimens and the thickness of the actual tissue, referring to the outside layer in the apical segment (Fig. 4a); discrepancies in height in the second moment of inertia clearly affected the result.

With increasing density, the modulus of elasticity is also increasing, which correlates with the different layers across the cross-section (Chave *et al.* 2009) (Fig. 6b).

The increasing structural moduli of elasticity of the segments was not a contradiction to decreasing Young's moduli of specimens, since the structural modulus of elasticity assumed that there was homogeneous material in cross-section. However, the decrease of moduli of elasticity in the bending tests may be an artefact, because a clear

discrimination between the outside and transition layer in the apical segments is not possible. The authors would expect an increase of rigidity with decreasing diameters of the vascular bundles, as previously observed in flax and further non-lignified plant fibers (Baley 2002; Munawar *et al.* 2007; Charlet *et al.* 2009). In addition, the transition and inside layers remained virtually unchanged along the rachis, pointing at similar material properties within its layers over the entire rachis.

In comparison, the modulus of elasticity of the outside layer was comparable to some hard- or softwood such as black walnut or larch (Niklas 1992), while that of the inside layer (3.7 GPa) was lower than balsa (Meier 2018). Considering the stress distribution during bending, *i.e.* maximum stresses in the periphery, the evolution yielded the stiffest material at the location where it unfolded its maximum resistance. Comparison of the mechanical properties of other palm rachises was difficult since values for the modulus of elasticity was only found for two very small species, *Chamaedorea erumpens* and *Rhapis excelsa* (these rachises have triangular cross-sections and side lengths below 10 mm) with only 118 MPa and 31 MPa (Niklas 1991), twentyfold less than the *Raphia* rachis studied here. The authors were unable to find any price information for rachises, as no technical use for these has been described yet.

The materials taken from arborescent palm stems can encompass the full range of densities and modulus of elasticity for all wood (Rich 1987). These values are highest in the periphery and towards the base; *e.g.* for *Iriartea gigantea*, up to 31 GPa with a density of dried specimens of  $1.0 \text{ gcm}^{-3}$  in the peripheral tissue of a 26 m tall plant (Rich 1987b) or up to 3.8 GPa with a dry density of  $0.5 \text{ gcm}^{-3}$  in the peripheral tissue for a 6 m tall *Cocos nucifera*. This holds true for higher vascular bundle densities than central tissues (Kuo-Huang *et al.* 2004). Niklas (1991) concluded that the rachis could be seen as a functional equivalent to a branch, since leaflets can function as simple leaves, and both involve a substantial investment in mechanical support tissues. The taper of a petiole provides an axial gradient regarding the second moment of area, while gradual differences in the fiber volume content and fiber distribution within the petiole provide an anatomical cause for differences in the modulus of elasticity measured along the rachis (Niklas 1991).

### Compression tests

The determination of compressive rigidity, also given by modulus of elasticity, exhibited a substantial difference between samples from the outer zone (outside and transition layer) and inside tissue of the rachis cross-section. The average value decreased from  $586 \pm 57 \text{ MPa}$  in the outer zone to  $96 \pm 49 \text{ MPa}$  in the center. There was no clear decrease or increase along the rachis.

The compression test described the properties of parenchyma with embedded fiber bundles. From an engineering point of view, the rachis is a tubular-like structure with a stiff outer wall surrounding a soft inner material. The inner material acts as a filler to prevent Euler buckling of the outer wall upon bending (Karam and Gibson 1995). Hence, mechanical properties and density are correlated (Niklas 1993a), as the parenchyma's modulus of elasticity is low, corresponding to low density.

### Tension tests

The tensile modulus, tensile strength, and breaking strain of 30 samples from six dry fiber bundles of the third segment were  $13.4 \pm 2.3 \text{ GPa}$ ,  $271 \pm 99 \text{ N/mm}^2$ , and  $2.67 \pm 0.52\%$ , respectively. No gradients were evaluated because the extraction of the vascular bundles from the outer and the transition layer was not possible.

Faruk *et al.* (2012) and Pickering *et al.* (2016) provided two comprehensive reviews of material properties of natural fibers, which made it possible to rank the obtained values. Compared to other natural fibers, *Raphia matombe* had a rather low tensile modulus similar to the lowest given value of jute (Pickering *et al.* 2016) or sisal, curaua, and bamboo fibers (Faruk *et al.* 2012). The tensile strength was rather low and was comparable to coir or wool fibers (Pickering *et al.* 2016), whereas the breaking strain ranges among ramie and flax (Faruk *et al.* 2012, Pickering *et al.* 2016).

#### *Specific modulus of elasticity*

Density decreased strongly from the outside layer to the inside layer, but there was no gradient along the rachis. Materials with higher density correspondingly displayed a higher density of fiber bundles and a higher modulus of elasticity. Increases in modulus of elasticity, modulus of rupture, and density are strongly positively correlated in palm stems (Rich 1987) or other plants and tissues (Niklas 1993a,b).

Giving the specific modulus of elasticity, the outside layer can easily compete with hardwood (Table 1) and, in average, may range up to 78% of the specific modulus of elasticity of steel. Therefore, *Raphia* would serve as an excellent construction material, if only the outside layer would be used. Nevertheless, it would be waste of material, and the rachises are a natural sandwich-beam-construction. The outside layer sustains tensile and compressive forces, whilst the core bear shear forces. However, carpenters seek to understand the characteristics of a material and use the material best fit for the purpose at hand. The gradual transition between the stiff outside and soft center guarantees a smooth stress distribution with high damage tolerance. The challenge is to process the surfaces of the inside layer due to its softness.

Since the rachis further is a very fast-growing renewable and locally abundant material, which offers a high aesthetic value, it can be recommended as a wood substitute in certain purposes. However, detailed studies on the number of leaves produced per year are still lacking. This should be investigated to ensure the sustainable exploitation of this strongly used natural resource.

**Table 1.** Density, Modulus of elasticity, and Specific Modulus of Elasticity of *Raphia*, Spruce Wood (*Picea glauca*), Beech Wood (*Fagus americana*), and Stainless Steel

Specimen, Species	Dry Density (kgm <sup>-3</sup> )	Modulus of elasticity (GPa)	Specific Modulus of elasticity (MPa/kgm <sup>-3</sup> )
<i>Raphia</i> outside	607 (±138)	11.2 (±1.4)	19.0
<i>Raphia</i> inside	194 (±52)	2.5 (±0.3)	12.2
Spruce wood	431*	9.8*	22.8
Beech wood	655*	11.6*	17.7
Stainless steel	7750**	190.3**	24.5

\*Niklas 1992, \*\*Engineers Edge 2000-2014.

## CONCLUSIONS

1. The bending and compression modulus of elasticity were highest toward the base and periphery of the very large leaf rachis of *Raphia matombe*.

2. The rachis showed a heterogeneous tissue distribution with a dry density varying from 194 to 607 kgm<sup>-3</sup>. Furthermore, the specific modulus of elasticity of the outer part of the rachis (19.0 MPa/kgm<sup>-3</sup>) is widely comparable with wood (*Picea glauca*, *Fagus americana*).
3. Due to the high morphological, anatomical, and mechanical heterogeneity of the rachis, it cannot necessarily be processed quickly and easily and but can be recommended as wood substitute in certain purposes.
4. We herewith can confirm that local people in northern Angola use this natural material in an adequate manner: when more load on the furniture piece is expected, more of the outer parts of the rachis are used for construction, *i.e.* for stools, beds, or baskets.

## ACKNOWLEDGMENTS

The University Kimpa Vita, Uíge, Angola, was an essential base for operations and provided logistical support. The authors thank Thomas Couvreur for the identification of the *Raphia* species and Markus Günther for conducting SEM studies. The fieldwork in Angola was supported by a travel fund from the German Academic Exchange Service (DAAD) and the program “Strategic Partnerships” of the TU Dresden. These published results were obtained in collaboration with the Instituto Nacional da Biodiversidade e Áreas de Conservação (INBAC) of the Ministério do Ambiente da República de Angola. We acknowledge support by the Open Access Publication Funds of the SLUB/TU Dresden.

## REFERENCES CITED

- Baley, C. (2002). “Analysis of the flax fibres tensile behaviour and analysis of the tensile stiffness increase,” *Composites Part A: Applied Science and Manufacturing* 33(7), 939-948. DOI: 10.1016/S1359-835X(02)00040-4
- Charlet, K., Eve, S., Jernot, J. P., Gomina, M., and Breard, J. (2009). “Tensile deformation of a flax fiber,” *Procedia Engineering* 1(1), 233-236. DOI: 10.1016/j.proeng.2009.06.055
- Chave, J., Coomes, D., Jansen, S., Lewis, S. L., Swenson, N. G., and Zanne, A. E. (2009). “Towards a worldwide wood economics spectrum,” *Ecology letters* 12(4), 351-366. DOI: 10.1111/j.1461-0248.2009.01285.x
- Engineers Edge (2000-2014), “Modulus of elasticity, Young’s modulus, average properties of structural materials, shear modulus, Poisson’s ratio, density,” ([http://www.engineersedge.com/manufacturing\\_spec/average\\_properties\\_structural\\_materials.htm](http://www.engineersedge.com/manufacturing_spec/average_properties_structural_materials.htm)), Accessed 17 December 2018.
- Faruk, O., Bledzki, A. K., Fink, H. P., and Sain, M. (2012). “Biocomposites reinforced with natural fibers: 2000–2010,” *Progress in Polymer Science* 37(11), 1552-1596. DOI: 10.1016/j.progpolymsci.2012.04.003
- Karam, G. N., and Gibson, L. J. (1995). “Elastic buckling of cylindrical shells with elastic cores—I. Analysis,” *International Journal of Solids and Structures* 32(8-9), 1259-1283. DOI: 10.1016/0020-7683(94)00147-O
- Killmann, K. (1983). “Some physical properties of the coconut palm stem,” *Wood Sci. Technol.* 17, 167-185.

- Kuerschner, K., and Hoffer, A. (1931). "Eine neue quantitative Cellulosebestimmung (A new method of cellulose determination)," *Chemiker Zeitung* 55, 161-168.
- Kuo-Huang, L. L., Huang, Y. S., Chen, S. S., and Huang, Y. R. (2004). "Growth stresses and related anatomical characteristics in coconut palm trees," *IAWA Journal* 25(3), 297-310. DOI: 10.1163/22941932-90000367
- Lautenschläger, T., Monizi, M., Pedro, M., Mandombe, J. L., Bránquima, M. F., Heinze, C., and Neinhuis, C. (2018). "First large-scale ethnobotanical survey in the province of Uíge, northern Angola," *Journal of Ethnobiology and Ethnomedicine* 14(51). DOI: 10.1186/s13002-018-0238-3
- Monizi, M., Mayawa, V., Fernando, J., Neinhuis, C., Lautenschläger, T., and Ngbolua, K.-T.-N. (2018a). "The cultural and socio-economic role of raffia palm wine in Uíge Province, Angola," *Discovery* 54(268), 119-129.
- Monizi, M., Julio, F., Ndiku, L., Ngbolua, K., Neinhuis, C., Lautenschläger, T., Luyeye, F. L., and Timoteo, H. M. (2018b). "Traditional knowledge and skills in rural Bakongo communities: A case study in the Uíge province, Angola," *American Journal of Environment and Sustainable Development* 3(3), 33-45.
- Meier, E. (2018): "The Wood Database," (<https://www.wood-database.com/balsa/>), Accessed 17 December 2018
- Munawar, S. S., Umemura, K., and Kawai, S. (2007). "Characterization of the morphological, physical, and mechanical properties of seven nonwood plant fiber bundles," *Journal of Wood Science* 53(2), 108-113. DOI:10.1007/s10086-006-0836-x
- Niklas, K. (1991). "Flexural stiffness allometries of angiosperm and fern petioles and rachises: Evidence for biomechanical convergence," *Evolution* 45(3), 734-750. DOI: 10.2307/2409924
- Niklas, K. J. (1992). "*Plant Biomechanics: An Engineering Approach to Plant Form and Function*," University of Chicago Press, Chicago, IL.
- Niklas, K. J. (1993a). "Influence of tissue density-specific mechanical properties on the scaling of plant height," *Annals of Botany* 72(2), 173-179. DOI: 10.1006/anbo.1993.1096
- Niklas, K. J. (1993b). "The scaling of plant height: A comparison among major plant clades and anatomical grades," *Annals of Botany* 72(2), 165-172. DOI: 10.1006/anbo.1993.1095
- Parthasarathy, M. V., and Klotz, L. H. (1976). "Palm 'Wood' I. Anatomical aspects," *Wood Science and Technology* 10(3), 215-229. DOI: 10.1007/BF00350831
- Pickering, K. L., Efendy, M. G. A., and Le, T. M. (2016). "A review of recent developments in natural fibre composites and their mechanical performance," *Composites Part A: Applied Science and Manufacturing* 83, 98-112. DOI: 10.1016/j.compositesa.2015.08.038
- Rich, P. M. (1987a). "Developmental anatomy of the stem of *Welfia georgii*, *Iriarteia gigantea*, and other arborescent palms—Implications for mechanical support," *American Journal of Botany* 74(6), 792-802. DOI: 10.2307/2443860
- Rich, P. M. (1987b). "Mechanical structure of the stem of arborescent palms," *Botanical Gazette* 148(1), 42-50. DOI: 10.1086/337626
- Rüggeberg, M., Speck, T., Paris, O., Lapiere, C., Pollet, B., Koch, G., and Burgert, I. (2008). "Stiffness gradients in vascular bundles of the palm *Washingtonia robusta*," *Proceedings of the Royal Society B: Biological Sciences* 275(1648), 2221-2229. DOI: 10.1098/rspb.2008.0531

Theander, O., and Westerlund, E. A. (1986). "Studies on dietary fiber. 3. Improved procedures for analysis of dietary fiber," *Journal of Agricultural and Food Chemistry* 34(2), 330-336. DOI: 10.1021/jf00068a045

Tomlinson, P. B. (2006). "The uniqueness of palms," *Botanical Journal of the Linnean Society* 151(1), 5-14. DOI: 10.1111/j.1095-8339.2006.00520.x

Article submitted: January 8, 2019; Peer review completed: February 10, 2019; Revised version received and accepted: March 4, 2019; Published: March 7, 2019.

DOI: 10.15376/biores.14.2.3364-3378